TEKNIK

Tersedia online di: http://ejournal.undip.ac.id/index.php/teknik

TEKNIK, 46 (2), 2025, 103-113

Evaluation of Liquefaction Potential in the Budong-Budong Dam Foundation Plan to Prevent Dam Failure Due to Liquefaction Using a Deterministic Approach

Dicky Erista *, Sukamta

Department of Civil Engineering, Faculty of Engineering, Diponegoro University,
Jl. Prof. Soedarto, SH, Tembalang, Semarang, Indonesia 50275

Abstract

The Budong-Budong Dam, located in the district of Central Mamuju, West Sulawesi Province, is currently under construction. The foundation plan of the dam is a layer of river deposits (alluvial) with a thickness of 25 m and a shallow water table depth, which has been shown to have liquefaction potential. This study aims to assess the liquefaction potential of the river deposit layer using some additional SPT test data. This research is expected to confirm the liquefaction potential of the river deposits layer so that it can be considered by the dam owner in determining the foundation excavation limit and prevent dam failure due to liquefaction. The liquefaction potential analysis was carried out using a semi-empirical procedure according to Idriss and Boulanger (2006). The analysis was performed under 2 (two) earthquake conditions, namely Operating Basis Earthquake (OBE) and Safety Evaluation Earthquake (SEE), using different values of fines content (5%, 15%, 35%) and earthquake magnitudes (6.8, 7.0, 7.3, 7.5 and 7.7). The analysis shows that the foundation plan of the Budong-Budong Dam has the potential for liquefaction under both OBE and SEE conditions, which generally occurs at a depth of about 10-12 m from the ground surface. The liquefaction potential of finer-grained river deposits tends to be lower.

Keyword : *engineering*; *Budong-Budong dam; liquefaction; river deposit foundation*

1. Introduction

Indonesia experiences a high amount of seismic activity due to its location, which is surrounded by four major tectonic plates. As a result, Indonesia experiences a high frequency of tectonic earthquakes. Between 1907 and 2016, Indonesia experienced 51,855 earthquakes with a magnitude (M_w) of 4.5 or higher (PuSGeN, 2017). Earthquakes, in addition to damaging buildings, bridges, and water structures such as dams (Lokananta & Susilo, 2018), can cause liquefaction in saturated sandy soil, resulting in more severe damage. Liquefaction can result in excessive soil deformation, both vertical and horizontal.

Several dams have been reported to have failed due to earthquake-induced liquefaction, including the Sheffield Dam in California, which failed as a result of the Santa Barbara M_w 6.5 earthquake in 1925 (Seed et al., 1969), and the Lower San Fernando Dam in California, which experienced a landslide on its upstream slope as a result of liquefaction caused by the San Fernando M_w 6.6 earthquake in 1971 (Seed et al., 1973). In Indonesia, there have never been occurrences of dam failure due to liquefaction. The liquefaction event that temporarily drew the world's attention was the liquefaction in Palu and its surrounding areas caused by the Palu-Donggala earthquake in 2018, which had a magnitude of 7.5 (Kusuma, 2020; Mason et al., 2021). Several regions in Majene Regency, West Sulawesi Province, were also reported to have undergone liquefaction as a result of the M_w 5.9 and 6.2 earthquakes in 2021 (Yuwana & Buana, 2021).

The Budong-Budong Dam, located in the Central Mamuju Regency of West Sulawesi Province, is now under construction on the Salulebo River, a tributary of the Budong-Budong River. Regionally, the dam site is flanked by many active faults, including the Palu Koro fault in the north and the Makassar Strait fault in the southwest, making it susceptible to earthquakes. Figure 1 depicts the location of the Budong-Budong Dam construction site.

According to the design report, the river deposits (alluvial) in the Salulebo River are holocene in age and consist of sandy and gravelly soil with a thickness of around 25 m and a groundwater table depth of about 2 m. According to Youd and Perkins (1978), holocene river courses are highly susceptible to liquefaction. Furthermore, soil strata with a shallow

*) Correspondence Author.
E-mail: dicky.erista@gmail.com

doi: 10.14710/teknik.v46i2.67803

groundwater table (less than 3 m) are highly susceptible to liquefaction (Youd et al., 1978). These characteristics could be an early indicator of probable liquefaction in the alluvial layers at the Budong-Budong Dam foundation, which is intended to serve as the foundation for the shoulder zones of the dam's upstream and downstream sections, respectively.

Research undertaken by dam owners during the planning stage further supports the possibility of liquefaction. The liquefaction potential investigation was conducted using SPT data. The study indicated that the river deposit layer at the Budong-Budong Dam foundation is susceptible to liquefaction when shaken by a maximum design earthquake (MDE) with a recurrence time of 10,000 years and a peak ground acceleration value of 0.5 g (River Basin Organization for Sulawesi III Palu). Considering the potential liquefaction in the river deposit layer, the dam builders want to excavate all of the river deposit material at the dam site, ensuring that the entire dam body is supported by a breccia rock foundation. However, there are several issues associated with the excavation of the river deposit layer, including the large volume of river deposit material to be excavated, which will necessitate a longer working time, the possibility of slope stability issues, and difficulties dewatering the riverbed during construction. Furthermore, the restricted disposal space for excavated river debris presents a difficulty that dam owners must address.

The potential for liquefaction in the river sediment layers located beneath the dam foundation will be evaluated in this study using additional SPT test data and analysis procedures that were not considered in previous liquefaction potential studies. This research aims to estimate the liquefaction potential in the river sediment layers, which can serve as a consideration for dam builders in determining the excavation limits for the foundation of the Budong-Budong Dam, as well as to prevent dam failure due to liquefaction.

2. Materials and Method

2.1 Required Data

The data required to analyze the potential liquefaction in the river deposit layer at the Budong-Budong Dam include standard penetration test (SPT) data, geological and geotechnical investigation data, river deposit material gradation data, and peak ground acceleration data at the research location.

SPT data on the river deposit layer was obtained from 3 (three) SPT tests, namely borehole BD-02 with a test depth of 16 m, borehole BH-01 with a test depth of 18 m, and borehole BH-05 with a test depth of 14 m. The borehole points BD-02 and BH-01 are located in the middle or axis of the dam, while the borehole point BH-05 is located in the downstream section of the dam. The depth of groundwater measured in each borehole is 2 m from the ground surface. The SPT test results at the three borehole locations can be seen in Figure 2. The SPT test results at the borehole BD-02 are shown in Figure 2a, while the SPT test results at boreholes BH-01 and BH-05 are shown in Figure 2b and Figure 2c, respectively.

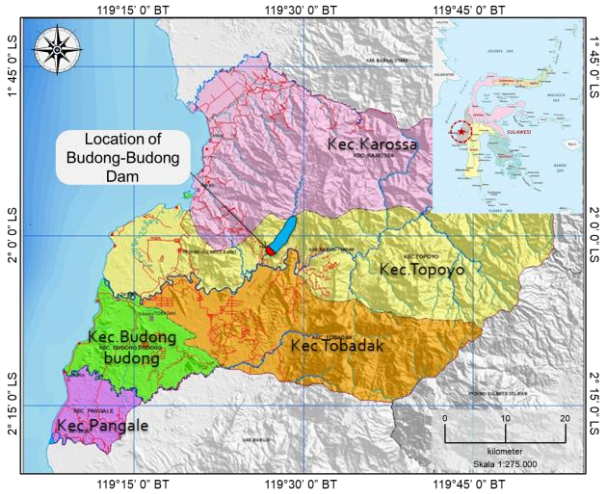

Figure 1. Map of the Budong-Budong Dam construction site.

In Figure 2a, it can be seen that the *N* SPT value starts from a depth of 14 m and reaches 50, indicating that the density of that layer is classified as dense. In Figure 2b, the N SPT value at the BH-01 borehole point has reached more than 50 starting from a depth of 6 m, but at a depth of 16 m, the measured *N* SPT value is relatively low at 4. At a depth of 18 m, the *N* SPT value significantly increased to 60. The low SPT value at a depth of 16 m may indicate the presence of a soil layer with very loose density properties at that depth. The existence of the very loose soil layer needs to be re-examined through drilling results at other borehole points near BH-01. Similarly, at the BH-01 borehole site, the *N* SPT value at the BH-05 borehole site has also reached more than 50 at a depth of 8 m, as shown in Figure 2c.

Peak Ground Acceleration (PGA) data is required to calculate the Cyclic Stress Ratio (CSR) acting on the soil. In this study, the peak ground acceleration was determined probabilistically from the Indonesian Earthquake Source and Hazard Map of 2017 (see Figure 3, Figure 4, and Figure 5). The PGA values used are based on the dam design earthquake criteria, namely the Operating Basis Earthquake (OBE) with a recurrence period of 145 years (ICOLD, 2016) and the Safety Evaluation Earthquake (SEE) with a recurrence period of 10,000 years.

The 2017 Indonesian Earthquake Source and Hazard Map only shows peak ground acceleration values at bedrock (SB). To obtain the peak ground acceleration values at the ground surface, the peak ground acceleration values at the bedrock must be

doi: 10.14710/teknik.v46i2.67803

corrected for the amplification factor (F_{PGA}), which is affected by local soil/rock conditions. The amplification factor and local soil/rock conditions are determined using SNI 8460:2017 for Geotechnical Design Requirements, as indicated in Table 1. This study examines the amplification factor of local soil/rock using SPT data.

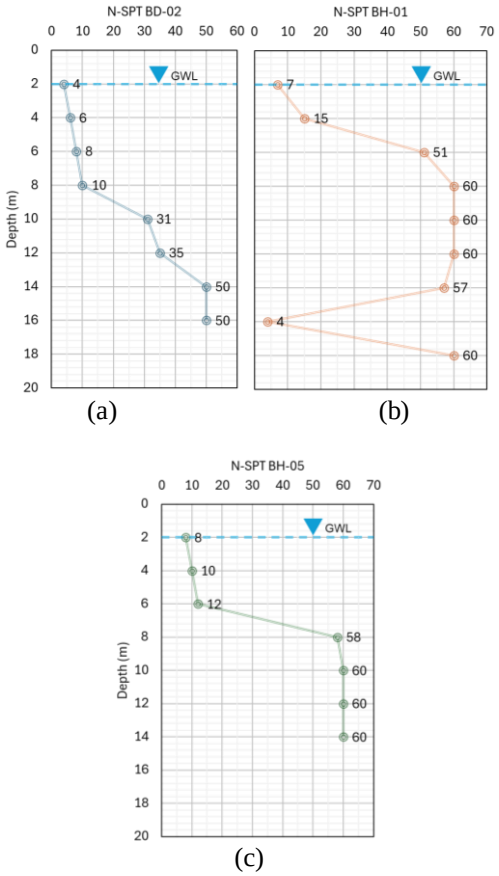

Figure 2. Standard penetration test (SPT) data. (a) borehole BD-02, (b) borehole BH-01, (c) borhole BH-05

2.2 Research Methodology

The first stage of this research is to gather the relevant data. The data used in the analysis were obtained from secondary sources such as the Budong-Budong Dam design report and geological and geotechnical investigation reports from the construction phase. This study assumes gradation data and fine content (*FC*) of river deposits, with *FC* values ranging from 5%, 15%, and 35% and considered constant at each depth. The *FC* value is selected in accordance division or categorization by Idriss dan Boulanger (2006, 2008).

Table 1. Amplification factor according to site class based on N-SPT value (SNI 8460:2017)

Site class	N-SPT	PGA				
		≤ 0.1	0.2	0.3	0.4	≥ 0.5
SA	-	0.8	0.8	0.8	0.8	0.8
SB	-	1.0	1.0	1.0	1.0	1.0
SC	>50	1.2	1.2	1.1	1.0	1.0
SD	15-50	1.6	1.4	1.2	1.1	1.0
SE	<15	2.5	1.7	1.2	0.9	0.9
SE	SS	SS	SS	SS	SS	SS

SPT data before analysis needs to be processed first by correcting the tool and test procedure factors, which include correction factors for energy ratio (C_E), borehole diameter (C_B), rod length (C_R), and soil sampler (C_S). The determination of correction factors for SPT tools and procedures refers to (Idriss dan Boulanger, 2008). In addition to these factors, SPT values also need to be corrected for effective vertical stress (C_N). The determination of the C_N value refers to (Idriss & Boulanger, 2006). The corrected SPT value is usually expressed as $(N_1)_{60}$. Subsequently, the calculation of the $(N_1)_{60}$ value equivalent to clean sand, expressed as $(N_1)_{60cs}$, is performed using the equation from (Idriss & Boulanger (2006) as presented in equations 6 and 7.

The potential for liquefaction is analyzed using the simplification procedure developed by Seed & Idriss (1971), which involves comparing the cyclic resistance ratio (CRR) of the soil with the cyclic stress ratio (CSR). If the CSR value caused by an earthquake is greater than the CRR value of soil, then the soil has the potential to experience liquefaction (FK < 1) and vice versa. In this study, the values of CSR and CRR are calculated using the equations from Idriss & Boulanger (2006), which are revisions of the Seed & Idriss (1971) equations. In their research, Mase (2018) and Zakariya et al. (2022) also used the equations from Idriss & Boulanger (2006). CSR can be calculated using equation 1, while CRR can be calculated using equation 5.

$$CSR = (\tau_{av}/\sigma'_v) = 0.65\,(a_{max}/g)(\,\sigma_v/\sigma'_v)r_d \quad (1)$$

$$r_d = \exp(\alpha(z) + \beta(z)\,M) \quad (2)$$

$$\alpha(z) = -1.012 - 1.126\sin\left(\frac{z}{11.73} + 5.133\right) \quad (3)$$

$$\beta(z) = 0.106 + 0.118\sin\left(\frac{z}{11.28} + 5.142\right) \quad (4)$$

with a_{max} is peak ground acceleration at ground surface (g), g is gravitational acceleration, σ_v is total stress of soil (kPa), σ'_v is effective vertical stress of soil (kPa), r_d is shear stress reduction coefficient, and z is the depth of soil being examined (m).

$$CRR_{M=7.5,\,\sigma'_{v}=1} = \exp\left(\frac{(N_1)_{60cs}}{14.1} + \left(\frac{(N_1)_{60cs}}{126}\right)^2 - \left(\frac{(N_1)_{60cs}}{23.6}\right)^3 + \left(\frac{(N_1)_{60cs}}{25.4}\right)^4 - 2.8\right) \quad (5)$$

$$(N_1)_{60cs} = (N_1)_{60} + \Delta\,(N_1)_{60} \quad (6)$$

$$\Delta(N_1)_{60} = \exp\left(1.63 + \frac{9.7}{FC+0.01} - \left(\frac{15.7}{FC+0.01}\right)^2\right) \quad (7)$$

with $(N_1)_{60cs}$ is equivalent clean sand corrected standard penetration and *FC* is fine content (%).

The CRR in equation 5 considers a magnitude (M_w) of 7.5 and an effective vertical stress (σ'_v) of 1 atm

doi: 10.14710/teknik.v46i2.67803

(101 kPa). To apply for M_w greater or less than 7.5, the CRR value needs to be corrected for the magnitude scaling factor (MSF). For σ'_v values greater or less than 1 atm, the CRR value needs to be corrected for the overburden correction factor (K_σ), which is influenced by the soil resistance value and can be expressed as $(N_1)_{60cs}$. MSF and K_σ were calculated using equations 8 to 9 from Idriss & Boulanger (2006).

$$\text{MSF} = 6.9 \exp\left(\frac{-M}{4}\right) - 0.058 \leq 1.8 \quad (8)$$

$$K_\sigma = 1 - C_\sigma \ln\left(\frac{\sigma'_v}{P_a}\right) \leq 1.1 \quad (9)$$

$$C_\sigma = \frac{1}{18.9 - 2.55\sqrt{(N_1)_{60}}} \leq 0.3 \quad (10)$$

with M is earthquake magnitude (M_w), σ'_v is effective vertical stress of soil (kPa), Pa is atmospheric pressure (1 atm equal to 100 kPa), and C_σ is the coefficient K_σ related to the value $(N_1)_{60}$.

The CRR at a specific earthquake magnitude and effective vertical stress can be calculated using equation 11. Next, the safety factor against potential liquefaction can be calculated using equation 12.

$$CRR_{M,\sigma'v} = CRR_{M=7.5,\sigma'v=1} \,.\, MSF.\, K_\sigma \quad (11)$$

$$FS_{liq} = \frac{CRR_{M,\sigma'_v}}{CSR_{M,\sigma'_v}} \quad (12)$$

The $(N_1)_{60cs}$ value greater than 37.5 is considered very dense to experience liquefaction, thus deemed not to have the potential for liquefaction. Therefore, the CRR value is set at 2.0 for $(N_1)_{60cs} > 37.5$ (Idriss & Boulanger, 2008; Tarigan, 2022).

The liquefaction resistance of soil is influenced by the effective vertical stress on the soil. Effective vertical stress is calculated by subtracting the total vertical stress from the pore water pressure in the soil at the depth under consideration. Parameters required to calculate the total stress on the soil include the depth of the groundwater table, the unit weight (γ) of the soil, and the unit weight of water (γ_w = 10 kN/m³ or kPa). The unit weight of river deposit material is estimated empirically based on the fine content of material (Yoshida, 2018). The determination of the estimated unit weight of river deposit material can be seen in Table 2. The unit weight of river deposit material above and below the groundwater table is differentiated to determine the soil's effective stress value based on real field conditions.

The analysis of liquefaction potential in this study was conducted under two earthquake condition scenarios, namely the OBE and SEE earthquakes. In each scenario, varying *FC* values and earthquake magnitudes were used. The *FC* values used are 5%, 15%, and 35%, while the earthquake magnitudes (M_w) used are 6.8, 7.0, 7.3, 7.5, and 7.7. According to PuSGeN (2017), the maximum earthquake magnitude that can occur due to the activity of the Palu-Koro fault segments and the Makassar Strait fault ranges from 6.8 to 7.3. Thus, the selection of earthquake magnitude variations is in accordance with the estimated earthquake magnitude that may occur at the research location.

Table 2. Estimation of unit weight of soil based on fine content

Soil type	Unit weight (T/m³)		Fines content (%)
	Below GWL	Above GWL	
Surface soil	1.7	1.5	100
Clay	1.5	1.4	100
Silt	1.75	1.55	90
Sandy silt	1.8	1.6	70
Silty fine sand	1.8	1.6	50
Very fine sand or fine sand with silt fine sand	1.85	1.65	20
Fine sand	1.95	1.75	10
Medium sand	2.0	1.8	5
Coarse sand	2.0	1.8	0
Sandy gravel	2.1	1.9	0

3. Results and Discussion

3.1 Determination of PGA Value

The Indonesian Earthquake Source and Hazard Map of 2017 does not provide PGA values for a return period of 145 years. The determination of PGA values for the OBE condition with a return period of 145 years is done by interpolating the PGA values for return periods of 100 years and 200 years. The PGA value for the SEE condition with a return period of 10,000 years can be obtained directly from the Indonesian Earthquake Source and Hazard Map of 2017. The PGA value is then corrected for the amplification factor, which depends on the site class or local soil/rock conditions. Determination of the amplification factor based on the average SPT value available in the field. From the calculation results, the corrected average *N*-SPT value $(N_1)_{60}$ is obtained as 13, so the site class at the research location is classified as soft soil (SE). Subsequently, the amplification factor can be determined based on Table 1. The peak ground acceleration in the bedrock, the amplification factor, and the peak ground acceleration at the surface in the Budong-Budong Dam location are presented in Table 3.

Table 3. The peak ground acceleration value in the bedrock, amplification factor, and peak ground acceleration on the surface

Earthquake	Return period (year)	SB (g)	F_{PGA}	PGA (g)
OBE	100	0.10	2.50	0.25
	145	0.12	2.32	0.28
	200	0.15	2.10	0.32
SEE	10,000	0.50	0.9	0.45

doi: 10.14710/teknik.v46i2.67803

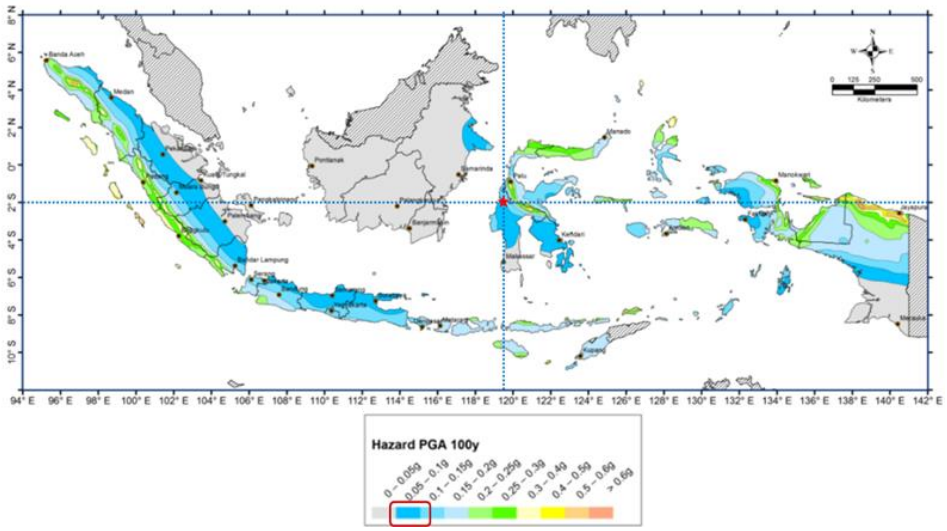

Figure 3. Map of peak ground acceleration in bedrock (SB) for a 100-year return period.

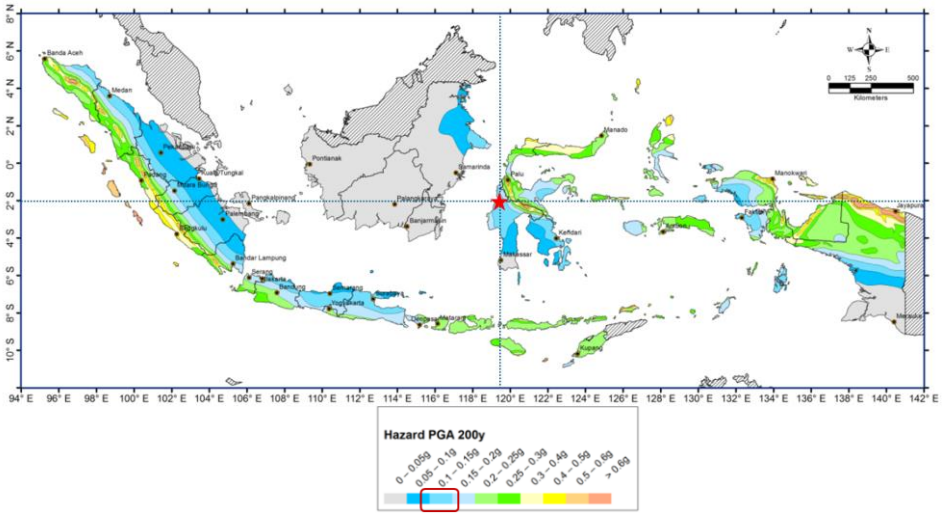

Figure 4. Map of peak ground acceleration in bedrock (SB) for a 200-year return period.

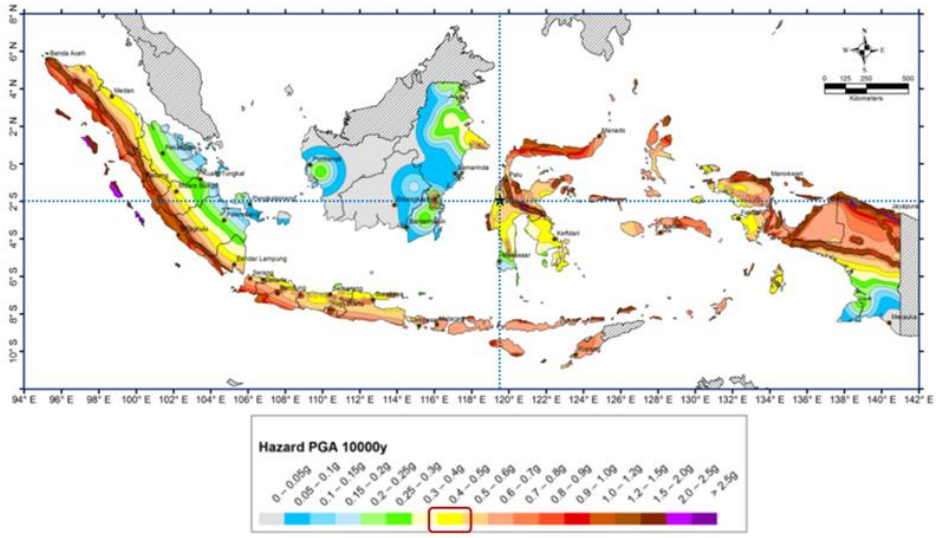

Figure 5. Map of peak ground acceleration in bedrock (SB) for a 10,000-year return period.

doi: 10.14710/teknik.v46i2.67803

3.2 Determination of Corrected SPT Value $(N_1)_{60}$

The value of vertical effective stress used to determine $(N_1)_{60}$ is calculated based on the unit weight (γ) of river deposit material and the depth of groundwater. The value of the unit weight of the river deposit material at each fine content is presented in Table 4. The groundwater depth at all borehole points is 2 m. The calculation of the $(N_1)_{60}$ value at points BD-02, BH-01, and BH-05 is presented in Table 5, Table 6, and Table 7, respectively.

Table 4. Unit weight of river deposit material (γ)

Berat isi	*FC*		
(kN/m^3)	5%	15%	35%
γ_{unsat} (di atas MAT)	18	17,5	16,5
γ_{sat} (di bawah MAT)	20	19,5	18,5

3.3 Safety factor against liquefaction potential

The safety factor for liquefaction potential at all SPT points, both under OBE and SEE conditions, as well as under various fine content and earthquake magnitudes, is presented in Table 8 and Table 9. The coloring of the safety factor values in the table is intended to indicate the presence or absence of liquefaction potential. The red color indicates that the safety factor is less than one (FS < 1), meaning the soil layer has the potential to experience liquefaction, while the green color indicates that the safety factor is greater than or equal to one (FS ≥ 1), meaning the soil layer does not have the potential to experience liquefaction.

Table 8 shows that generally river deposits will experience liquefaction up to a depth of 8 m under OBE conditions. At point BD-02, liquefaction has the potential to occur up to a depth of 12 m if shaken by an earthquake with a magnitude greater than or equal to 7.3 ($Mw \geq 7.3$) with a fine content value of 5%. Meanwhile, at points BH-01 and BH-05, liquefaction is only potentially possible up to depths of 4 m and 6 m, respectively, at various earthquake magnitude values. However, at point BH-01, liquefaction has the potential to occur at a depth of 16 m at various earthquake magnitude values and fine content. This is likely caused by the presence of a thin layer of soft soil at that depth. The presence of the soft soil layer needs to be reconfirmed through field investigation, considering that the presence of the soft soil layer was not detected by other nearby boreholes. Table 8 also shows that the potential for liquefaction tends to decrease in river sediment layers with a fine content of 35%.

Table 5. $(N_1)_{60}$ value for borehole BD-02

H (m)	σv (kPa)	u (kPa)	$\sigma' v$ (kPa)	N_m	C_E	C_R	C_B	C_S	N_{60}	C_N	$(N_1)_{60}$
2	36	0	36	4	0,85	0,75	1,00	1,00	2,55	1,70	4,3
4	76	20	56	6	0,85	0,80	1,00	1,00	4,08	1,42	5,8
6	116	40	76	8	0,85	0,85	1,00	1,00	5,78	1,17	6,8
8	156	60	96	10	0,85	0,95	1,00	1,00	8,08	1,02	8,3
10	196	80	116	31	0,85	0,95	1,00	1,00	25,03	0,94	23,6
12	236	100	136	35	0,85	1,00	1,00	1,00	29,75	0,89	26,4
14	276	120	156	50	0,85	1,00	1,00	1,00	42,50	0,87	36,9
16	316	140	176	50	0,85	1,00	1,00	1,00	42,50	0,83	35,3

Table 6. $(N_1)_{60}$ value for borehole BH-01

H (m)	σv (kPa)	u (kPa)	$\sigma' v$ (kPa)	N_m	C_E	C_R	C_B	C_S	N_{60}	C_N	$(N_1)_{60}$
2	36	0	36	4	0,85	0,75	1,00	1,00	2,55	1,70	4,3
4	76	20	56	6	0,85	0,80	1,00	1,00	4,08	1,42	5,8
6	116	40	76	8	0,85	0,85	1,00	1,00	5,78	1,17	6,8
8	156	60	96	10	0,85	0,95	1,00	1,00	8,08	1,02	8,3
10	196	80	116	31	0,85	0,95	1,00	1,00	25,03	0,94	23,6
12	236	100	136	35	0,85	1,00	1,00	1,00	29,75	0,89	26,4
14	276	120	156	50	0,85	1,00	1,00	1,00	42,50	0,87	36,9
16	316	140	176	50	0,85	1,00	1,00	1,00	42,50	0,83	35,3

Table 7. $(N_1)_{60}$ value for borehole BH-05

H (m)	σv (kPa)	u (kPa)	$\sigma' v$ (kPa)	N_m	C_E	C_R	C_B	C_S	N_{60}	C_N	$(N_1)_{60}$
2	36	0	36	8	0.85	0.75	1.00	1.00	5.10	1.70	8.7
4	76	20	56	10	0.85	0.80	1.00	1.00	6.80	1.37	9.3
6	116	40	76	12	0.85	0.85	1.00	1.00	8.67	1.16	10.1
8	156	60	96	58	0.85	0.95	1.00	1.00	46.84	1.01	47.3
10	196	80	116	60	0.85	0.95	1.00	1.00	48.45	0.96	46.6
12	236	100	136	60	0.85	1.00	1.00	1.00	51.00	0.92	47.0
14	276	120	156	60	0.85	1.00	1.00	1.00	51.00	0.89	45.3

doi: 10.14710/teknik.v46i2.67803

Table 8. The potential for liquefaction at all borehole points under OBE conditions with various fine contents and earthquake magnitudes

***FC* = 5%**

H	M_w 6.8			M_w 7.0			M_w 7.3			M_w 7.5			M_w 7.7		
m	BD-02	BH-01	BH-05	BD-02	BH-01	BH-05	BD-02	BH-01	BH-05	BD-02	BH-01	BH-05	BD-02	BH-01	BH-05
2	0.59	0.74	0.80	0.56	0.70	0.75	0.52	0.65	0.70	0.49	0.61	0.66	0.46	0.58	0.62
4	0.48	0.78	0.61	0.46	0.74	0.57	0.42	0.68	0.53	0.40	0.64	0.50	0.37	0.61	0.47
6	0.46	2.00	0.57	0.44	2.00	0.54	0.40	2.00	0.49	0.38	2.00	0.46	0.35	2.00	0.43
8	0.49	2.00	2.00	0.46	2.00	2.00	0.42	2.00	2.00	0.39	2.00	2.00	0.37	2.00	2.00
10	1.17	2.00	2.00	1.09	2.00	2.00	0.98	2.00	2.00	0.92	2.00	2.00	0.86	2.00	2.00
12	1.46	2.00	2.00	1.36	2.00	2.00	1.22	2.00	2.00	1.13	2.00	2.00	1.05	2.00	2.00
14	2.00	2.00	2.00	2.00	2.00	2.00	2.00	2.00	2.00	2.00	2.00	2.00	2.00	2.00	2.00
16	2.00	0.35		2.00	0.32		2.00	0.28		2.00	0.26		2.00	0.24	
18		2.00			2.00			2.00			2.00			2.00	

***FC* = 15%**

H	M_w 6.8			M_w 7.0			M_w 7.3			M_w 7.5			M_w 7.7		
m	BD-02	BH-01	BH-05	BD-02	BH-01	BH-05	BD-02	BH-01	BH-05	BD-02	BH-01	BH-05	BD-02	BH-01	BH-05
2	0.74	0.92	0.97	0.71	0.87	0.92	0.65	0.80	0.85	0.62	0.76	0.80	0.58	0.72	0.76
4	0.59	0.93	0.73	0.56	0.88	0.69	0.51	0.81	0.64	0.48	0.76	0.60	0.46	0.72	0.57
6	0.57	2.00	0.68	0.53	2.00	0.64	0.49	2.00	0.59	0.46	2.00	0.55	0.43	2.00	0.52
8	0.59	2.00	2.00	0.55	2.00	2.00	0.50	2.00	2.00	0.47	2.00	2.00	0.44	2.00	2.00
10	1.59	2.00	2.00	1.48	2.00	2.00	1.34	2.00	2.00	1.25	2.00	2.00	1.17	2.00	2.00
12	2.00	2.00	2.00	2.00	2.00	2.00	1.84	2.00	2.00	1.71	2.00	2.00	1.59	2.00	2.00
14	2.00	2.00	2.00	2.00	2.00	2.00	2.00	2.00	2.00	2.00	2.00	2.00	2.00	2.00	2.00
16	2.00	0.43		2.00	0.39		2.00	0.35		2.00	0.32		2.00	0.30	
18		2.00			2.00			2.00			2.00			2.00	

***FC* = 35%**

H	M_w 6.8			M_w 7.0			M_w 7.3			M_w 7.5			M_w 7.7		
m	BD-02	BH-01	BH-05	BD-02	BH-01	BH-05	BD-02	BH-01	BH-05	BD-02	BH-01	BH-05	BD-02	BH-01	BH-05
2	0.86	1.04	1.10	0.82	0.98	1.04	0.75	0.91	0.96	0.71	0.86	0.91	0.68	0.81	0.86
4	0.67	1.07	0.83	0.64	1.01	0.78	0.58	0.93	0.72	0.55	0.88	0.68	0.52	0.83	0.64
6	0.64	2.00	0.77	0.60	2.00	0.73	0.55	2.00	0.66	0.52	2.00	0.62	0.49	2.00	0.59
8	0.67	2.00	2.00	0.62	2.00	2.00	0.57	2.00	2.00	0.53	2.00	2.00	0.50	2.00	2.00
10	2.00	2.00	2.00	2.00	2.00	2.00	1.88	2.00	2.00	1.76	2.00	2.00	1.64	2.00	2.00
12	2.00	2.00	2.00	2.00	2.00	2.00	2.00	2.00	2.00	2.00	2.00	2.00	2.00	2.00	2.00
14	2.00	2.00	2.00	2.00	2.00	2.00	2.00	2.00	2.00	2.00	2.00	2.00	2.00	2.00	2.00
16	2.00	0.48		2.00	0.44		2.00	0.39		2.00	0.36		2.00	0.33	
18		2.00			2.00			2.00			2.00			2.00	

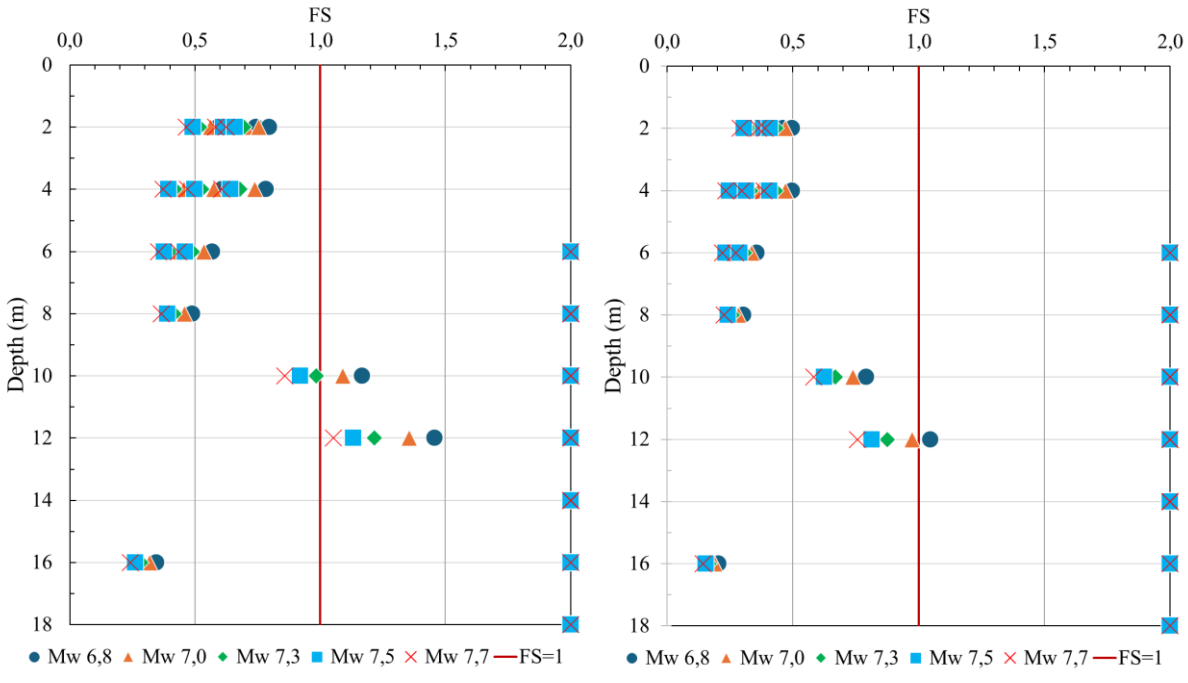

Figure 6. The potential for liquefaction at all borehole points under OBE and SEE conditions with fine content .(FC) 5% and various earthquake magnitudes (M_w). (a) OBE condition, (b) SEE condition.

doi: 10.14710/teknik.v46i2.67803

Table 9. The potential for liquefaction at all borehole points under SEE conditions with various fine contents and earthquake magnitudes

FC 5%

H	M_w 6.8			M_w 7.0			M_w 7.3			M_w 7.5			M_w 7.7		
m	BD-02	BH-01	BH-05	BD-02	BH-01	BH-05	BD-02	BH-01	BH-05	BD-02	BH-01	BH-05	BD-02	BH-01	BH-05
2	0.37	0.46	0.50	0.35	0.44	0.47	0.32	0.40	0.43	0.31	0.38	0.41	0.29	0.36	0.39
4	0.30	0.50	0.38	0.28	0.47	0.36	0.26	0.43	0.33	0.25	0.41	0.31	0.23	0.38	0.30
6	0.29	2.00	0.36	0.27	2.00	0.34	0.25	2.00	0.31	0.23	2.00	0.29	0.22	2.00	0.27
8	0.30	2.00	2.00	0.28	2.00	2.00	0.26	2.00	2.00	0.24	2.00	2.00	0.23	2.00	2.00
10	0.79	2.00	2.00	0.74	2.00	2.00	0.67	2.00	2.00	0.62	2.00	2.00	0.58	2.00	2.00
12	1.05	2.00	2.00	0.97	2.00	2.00	0.87	2.00	2.00	0.81	2.00	2.00	0.76	2.00	2.00
14	2.00	2.00	2.00	2.00	2.00	2.00	2.00	2.00	2.00	2.00	2.00	2.00	2.00	2.00	2.00
16	2.00	0.20		2.00	0.19		2.00	0.17		2.00	0.15		2.00	0.14	
18		2.00			2.00			2.00			2.00			2.00	

FC 15%

H	M_w 6.8			M_w 7.0			M_w 7.3			M_w 7.5			M_w 7.7		
m	BD-02	BH-01	BH-05	BD-02	BH-01	BH-05	BD-02	BH-01	BH-05	BD-02	BH-01	BH-05	BD-02	BH-01	BH-05
2	0.46	0.57	0.61	0.44	0.54	0.57	0.40	0.50	0.53	0.38	0.47	0.50	0.36	0.45	0.47
4	0.37	0.58	0.46	0.35	0.55	0.43	0.32	0.50	0.40	0.30	0.48	0.37	0.28	0.45	0.35
6	0.35	2.00	0.43	0.33	2.00	0.40	0.30	2.00	0.37	0.28	2.00	0.34	0.27	2.00	0.32
8	0.37	2.00	2.00	0.35	2.00	2.00	0.31	2.00	2.00	0.29	2.00	2.00	0.28	2.00	2.00
10	0.99	2.00	2.00	0.92	2.00	2.00	0.83	2.00	2.00	0.78	2.00	2.00	0.73	2.00	2.00
12	1.37	2.00	2.00	1.28	2.00	2.00	1.15	2.00	2.00	1.07	2.00	2.00	0.99	2.00	2.00
14	2.00	2.00	2.00	2.00	2.00	2.00	2.00	2.00	2.00	2.00	2.00	2.00	2.00	2.00	2.00
16	2.00	0.27		2.00	0.25		2.00	0.22		2.00	0.20		2.00	0.19	
18		2.00			2.00			2.00			2.00			2.00	

FC 35%

H	M_w 6.8			M_w 7.0			M_w 7.3			M_w 7.5			M_w 7.7		
m	BD-02	BH-01	BH-05	BD-02	BH-01	BH-05	BD-02	BH-01	BH-05	BD-02	BH-01	BH-05	BD-02	BH-01	BH-05
2	0.54	0.65	0.69	0.51	0.61	0.65	0.47	0.56	0.60	0.44	0.53	0.57	0.42	0.51	0.54
4	0.42	0.67	0.52	0.40	0.63	0.49	0.36	0.58	0.45	0.34	0.54	0.42	0.32	0.51	0.40
6	0.40	2.00	0.48	0.37	2.00	0.45	0.34	2.00	0.41	0.32	2.00	0.39	0.30	2.00	0.37
8	0.41	2.00	2.00	0.39	2.00	2.00	0.35	2.00	2.00	0.33	2.00	2.00	0.31	2.00	2.00
10	1.39	2.00	2.00	1.30	2.00	2.00	1.17	2.00	2.00	1.09	2.00	2.00	1.02	2.00	2.00
12	2.00	2.00	2.00	2.00	2.00	2.00	1.87	2.00	2.00	1.74	2.00	2.00	1.62	2.00	2.00
14	2.00	2.00	2.00	2.00	2.00	2.00	2.00	2.00	2.00	2.00	2.00	2.00	2.00	2.00	2.00
16	2.00	0.30		2.00	0.27		2.00	0.24		2.00	0.22		2.00	0.21	
18		2.00			2.00			2.00			2.00			2.00	

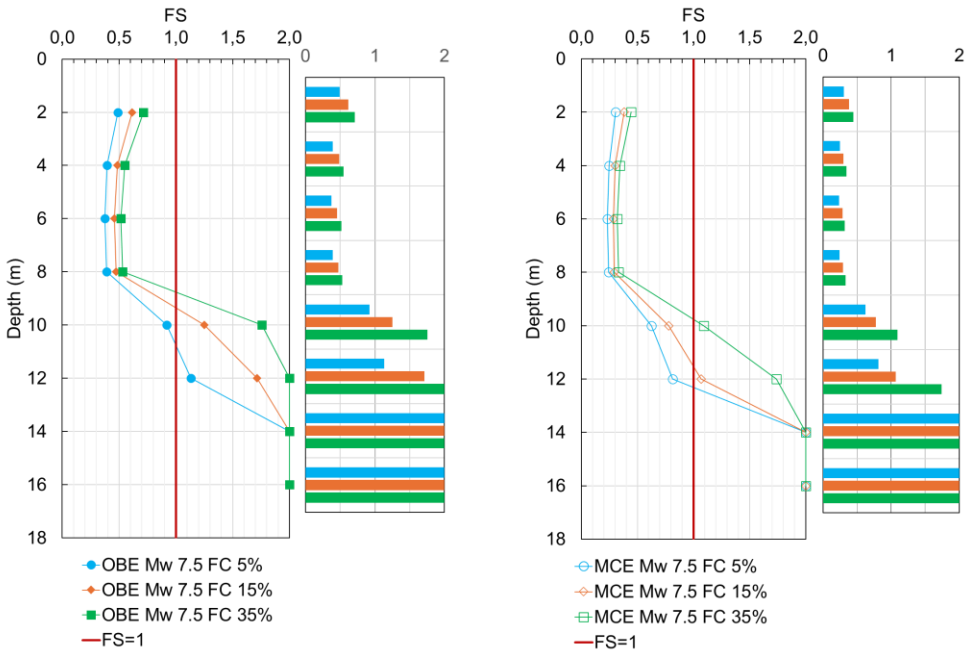

(a) (b)

Figure 7. The potential for liquefaction at point BD-02 with an earthquake magnitude of 7.5 and various fine content values (FC). (a) under OBE conditions, (b) under SEE conditions.

doi: 10.14710/teknik.v46i2.67803

Under SEE conditions, liquefaction has the potential to occur up to a depth of 12 m, especially at point BD-02 with a fine content of 5% and an earthquake magnitude of 7.0 or more, as shown in Table 9. The depth of soil that is potentially susceptible to liquefaction tends to decrease as the fine content increases. At a fine content value of 35%, liquefaction is only likely to occur up to a depth of 8 m.

The results of the liquefaction potential calculations are also presented in graphical form as shown in Figure 6 and Figure 7. Figure 6 presents a graph of the liquefaction potential safety factor in river sediment layers with a fine content of 5% at all borehole points with various earthquake magnitudes. Figure 6a and Figure 6b, respectively show the distribution of the safety factor under OBE and SEE conditions. The safety factor values on the left side of the FS = 1 line indicate that liquefaction is potentially occurring and vice versa. The graphs in Figure 6a and Figure 6b show that under OBE conditions, liquefaction generally occurs up to a depth of 8 m–10 m, whereas under SEE conditions, liquefaction occurs up to a depth of 12 m. The safety factor shows a significant decrease under SEE conditions, which generally have a value of less than 0.5 (FS < 0.5). This indicates that the greater the peak ground acceleration, the higher the potential for liquefaction, as shown in the studies conducted by Tarigan (2022) and Widyatmoko et al. (2023).

Figure 7 presents the liquefaction potential factor of safety values at borehole point BD-02 for a 7.5 magnitude earthquake with various fine content values. Figure 7a and Figure 7b, respectively show the factor of safety values under OBE and SEE conditions. The graph in Figure 7 shows how the fine content affects the potential liquefaction safety factor. The factor of safety against liquefaction potential decreases as the fine content in the river deposit decreases, both under OBE and SEE conditions. The clustered bar graphs in Figures 7a and 7b also clearly show that the safety factor decreases as the fine content decreases, leading to a higher potential for liquefaction.

In relation to the potential for liquefaction in the river deposit layer at the Budong-Budong Dam site, it is necessary to plan mitigation efforts for this liquefaction potential. According to the New Zealand Geotechnical Society & Ministry of Business, Innovation and Employment (2017), there are generally 5 (five) liquefaction mitigation techniques, namely the remove and replacement method, densification, solidification, reinforcement, and drainage. The stripping and replacement method is carried out by replacing soil layers that are prone to liquefaction with liquefaction-resistant materials such as well-graded compact gravel and soil-cement mixtures. The densification method aims to rearrange soil particles to form a denser configuration, thereby increasing the soil's density, shear strength, and resistance to liquefaction. The solidification method is carried out by mixing cement or additives into the soil pores in situ, thereby forming strong bonds between soil particles. The reinforcement method uses underground wall construction with a grid pattern. The drainage method consists of 2 (two) parts, namely (1) the installation of vertical water drains (prefabricated vertical drains) and (2) desaturation of soil with the potential for liquefaction by permanently lowering the groundwater table.

In principle, the dam foundation must have adequate bearing capacity, shear strength, and be safe against seepage (Department of Housing and Regional Infrastructure, 2003). Soil/rock layers usually need to be excavated to a certain depth to obtain a foundation that meets those requirements. River deposit layers are generally unconsolidated, making them less stable and prone to movement (Hasan, 2022). The relative density of river sediment layers also varies, where the surface layer is usually loose to somewhat dense, while the lower layer is dense, has low compressibility, and high shear strength (Fell et al., 2015). Considering these factors, the liquefaction mitigation effort deemed effective and efficient to be applied to the foundation of the Budong-Budong Dam is the excavation of the entire layer of river sediment that has the potential to liquefy, especially in the dam site area. In addition to aiming to mitigate dam failure due to liquefaction, the excavation of river sediment layers is also intended to obtain a foundation that meets the requirements.

4. Conclusion

The foundation plan of the Budong-Budong Dam, which consists of river deposit layers, has the potential to experience liquefaction under both OBE and SEE conditions, with depths reaching approximately 10–12 m from the ground surface. The fine content (*FC*) in river deposits, peak ground acceleration (PGA), and earthquake magnitude affect the soil's susceptibility to liquefaction. The lower the fine content, the lower the safety factor for liquefaction potential. Meanwhile, the higher the PGA value and earthquake magnitude, the lower the safety factor, thus increasing the potential for liquefaction. The mitigation efforts for liquefaction that are considered effective and efficient when applied to the foundation of the Budong-Budong Dam involve excavating all river deposit materials that have the potential to experience liquefaction, especially in the dam site area. The sampling of river deposit material along with the grading and index property tests should be conducted in future research. In addition, additional SPT testing combined with cone penetration tests on the river deposit layers is also recommended to be conducted in future research so that the liquefaction potential analysis can be carried out comprehensively, allowing for a more accurate estimation of the liquefaction potential for the Budong-Budong Dam foundation plan.

doi: 10.14710/teknik.v46i2.67803

Acknowledgment

The author expresses gratitude to River Basin Organization for Sulawesi III for their willingness to assist in providing the necessary data for this research, as well as to all parties who have contributed to the work and completion of this research.

References

National Standardization Agency of Indonesia. (2017). Indonesian National Standard (SNI) No. 8460:2017 About Geotechnical Design Requirements. Jakarta

River Basin Organization for Sulawesi III. (2018). Design Note Report - Design Certification, Model Test, and Advanced Geological Investigation of the Budong-Budong Dam, Central Mamuju Regency.

Departement of Housing and Regional Infrastructure. (2003). Guidelines for General Criteria for Dam Design.

Fell, R., MacGregor, P., Stapledon, D., Bell, G., & Foster, M. (2015). Geotechnical Engineering of Dams 2nd Edition. CRC Press.

Hasan, M. (2022). Analisis Endapan Aluvial dan Struktur Geologi di Daerah Bojonegoro dan Sekitarnya dengan Metode Resistivitas 2D dan Data Pemboran. Universitas Indonesia.

Idriss, I. M., & Boulanger, R. W. (2006). Semi-Empirical Procedures for Evaluating Liquefaction Potential During Earthquakes. *Soil Dynamics and Earthquake Engineering*, *26*(2–4), 115–130.

Idriss, M. I., & Boulanger, W. R. (2008). Soil Liquefaction During Earthquake. Earthquake Engineering Research Institute.

Kusuma, W. B. (2020). Analisa Kuantitatif dan Kualitatif Potensi Likuifaksi. *Majalah Ilmiah Swara Patra*, *10*(2), 5–16. https://doi.org/10.37525/sp/2020-2/251

Lokananta, R. D., & Susilo, A. J. (2018). Analisis Daya Dukung Tiang Aksial Dengan Mempertimbangkan Potensi Likuifaksi. *JMTS: Jurnal Mitra Teknik Sipil*, *1*(1), 281. https://doi.org/10.24912/jmts.v1i1.2268

Mase, L. Z. (2018). Studi Kehandalan Metode Analisis Likuifaksi Menggunakan SPT Akibat Gempa 8, 6 Mw, 12 September 2007 di Area Pesisir Kota Bengkulu. *Jurnal Teknik Sipil*, *25*(1), 53–60.

Mason, H. B., Montgomery, J., Gallant, A. P., Hutabarat, D., Reed, A. N., Wartman, J., Irsyam, M., Simatupang, P. T., Alatas, I. M., Prakoso, W. A., Djarwadi, D., Hanifa, R., Rahardjo, P., Faizal, L., Harnanto, D. S., Kawanda, A., Himawan, A., & Yasin, W. (2021). East Palu Valley Flowslides Induced by the 2018 M 7.5 Palu-Donggala Earthquake. *Geomorphology*, *373*, 107482. https://doi.org/10.1016/j.geomorph.2020.107482

New Zealand Geotechnical Society, & Ministry of Business, Innovation & Employment (2017). Earthquake Geotechnical Engineering Practice, Module 5 : Ground Improvement Soils Prone To Liquefaction.

Pusat Studi Gempa Nasional (PuSGeN). (2017). Peta Sumber dan Bahaya Gempa Indonesia Tahun 2017. Pusat Penelitian dan Pengembangan Perumahan dan Permukiman, Badan Penelitian dan Pengembangan, Kementerian Pekerjaan Umum dan Perumahan Rakyat.

Seed, B. H., Lee, K. L., & Idriss, I. M. (1969). Analysis of Sheffield Dam Failure. *Journal of the Soil Mechanics and Foundations Division*, *95*(6), 1453–1490. https://doi.org/10.1061/JSFEAQ.0001352

Seed, H. B., & Idriss, I. M. (1971). Simplified Procedure for Evaluating Soil Liquefaction Potential. *Journal of the Soil Mechanics and Foundations Division*, *97*(9), 1249–1273. https://doi.org/10.1061/JSFEAQ.0001662

Seed, H. B., K.L. Lee, I.M. Idriss, & F. Makdisi. (1973). Analysis of the Slides in the San Fernando Dams During the Earthquake of Feb. 9, 1971. *Earthquake Engineering Research Center*, *73–2*.

Tarigan, R. (2022). Kajian Potensi Likuifaksi Lapisan Tanah Menggunakan Metode Korelasi Empris Nilai CSR Dan CRR. *Jurnal Darma Agung*, *30*(1), 1. https://doi.org/10.46930/ojsuda.v30i1.1404

Widyatmoko, A., Legono, D., & Hardiyatmo, H. C. (2023). Liquefaction Potential Analysis Around Sediment Control Structure of Paneki River, Central Sulawesi. *AIP Conference Proceedings*, *2629*(1).

Yoshida, N. (2018). Remedial Measures Against Soil Liquefaction: from Investigation and Design to Implementation. Routledge.

Youd, T. L., & Perkins, D. M. (1978). Mapping Liquefaction-Induced Ground Failure Potential. *Journal of the Geotechnical Engineering Division*, *104*(4), 433–446. https://doi.org/10.1061/AJGEB6.0000612

Youd, T. L., Tinsley, J. C., Perkins, D. M., King, E. J., & Preston, R. (1978). Liquefaction Potential Map of San Fernando Valley, California. *Int. Conf. on Microzonation for Safer Construction, San Francisco*, 267–278.

Yuwana, D. A., & Buana, T. W. (2021). Manifestasi Likuefaksi dan Gerakan Tanah Akibat Gempa Bumi 14 Dan 15 Januari 2021 di Majene, Sulawesi Barat. *Geo Spatial Proceeding*.

Zakariya, A., Nurdiansyah, F., Galag, C. T. S. A., & Situmorang, J. (2022). Analisis Kuantitatif dan Kualitiatif Potensi Likuefaksi di Area Tanah Kepasiran Medium-Padat Dekat Sesar Opak. *Jurnal Jalan Jembatan*, *39*(2), 74–87.

